IPMCs as EAPs: Fundamentals

6

Kinji Asaka, Kwang Kim, Keisuke Oguro, and Mohsen Shahinpoor

Contents

Abstract

This chapter reviews the fundamentals of ionic polymer–metal composites (IPMCs), which are used for sensors and actuators. First, the basic structure of IPMCs is described, and a brief review of their development is provided. Then,

K. Asaka (✉)
Inorganic Functional Material Research Institute, National Institute of Advanced Industrial Science and Technology (AIST), Ikeda, Osaka, Japan
e-mail: asaka-kinji@aist.go.jp

K. Kim
Department of Mechanical Engineering, University of Nevada, Las Vegas, Las Vegas, NV, USA
e-mail: kwang.kim@unlv.edu

K. Oguro
National Institute of Advanced Industrial Science and Technology (AIST), Ikeda, Osaka, Japan
e-mail: oguro-keisuke@aist.go.jp

M. Shahinpoor
Biomedical Engineering/Advanced Robotics (BEAR) Laboratories, Department of Mechanical Engineering, Graduate School of Biomedical Science and Engineering, University of Maine, Orono, ME, USA
e-mail: shah@maine.edu

F. Carpi (ed.), *Electromechanically Active Polymers*, Polymers and Polymeric Composites: A Reference Series, DOI 10.1007/978-3-319-31530-0_6

the configurations of various devices based on them, including those of the electrode materials and ionic polymers, are described. Then, the basic techniques used to characterize IPMCs are described. In the next section, electromechanical models and, in particular, a physics-based model of an IPMC actuator are discussed. Finally, electrochemical models, including an Alternating Current impedance equivalent circuit model and an electrode reaction model, and a mechanical model are discussed.

Keywords
Ionic Polymer-Metal Composite (IPMC) • Ionic Polymer • Electrodes • Characterization • Electromechanical model • Nernst-Planck equation • Onsager relation • Electrochemical model • Impedance • Cyclic voltammetry • Mechanical model

1 General Introduction and Historical Review

Ionic polymer–metal composites (IPMCs), which are composed of an ionic polymer (IP) and metal electrodes, are one of the most promising electroactive polymer (EAP) materials for soft actuators and sensors. Known as bending actuators, IPMCs exhibit soft and extremely large bending motions in the presence of large ionic currents (Fig. 1).

Moreover, IPMCs are capable of large bending actuations when subjected to low voltages. When the voltage is applied, the counter cations move toward the cathode side with dragging water, resulting in a pressure gradient in the ionic gel polymer (Fig. 2).

In addition to their bending properties, IPMC actuators have a number of advantages that make them attractive for use in various biomedical and human affinity applications:

1. Low driving voltage (1–3 V)
2. Relatively high-frequency response (up to several hundred hertz)
3. Large displacement
4. Soft
5. Can be formed into any shape
6. Miniaturizable
7. Activatable in water or wet conditions as well as dry conditions

In addition to their actuation capabilities, IPMCs exhibit remarkable sensing properties. In particular, an electric current is generated in IPMCs in response to bending moments imposed on them; the generated voltage can be as high as tens of millivolts for large bending displacements. This property makes them suitable for use in soft mechanical sensors and energy harvesting systems.

Hamlen et al. were the first to report the direct transformation of electrical energy into mechanical work using an IP gel (Hamlen et al. 1965). Since 1965, many pioneering researchers have investigated the electric response of ionic gels (DeRossi

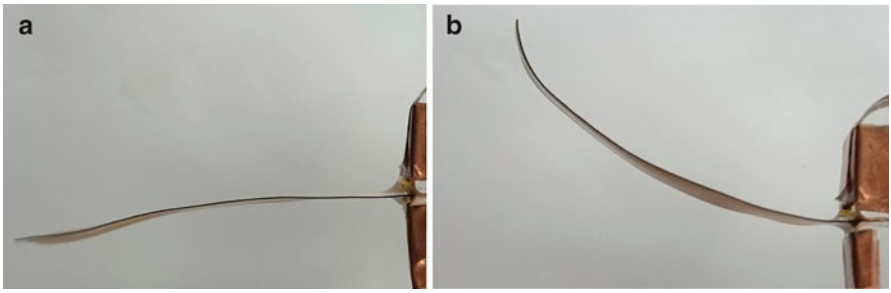

Fig. 1 Photograph showing the bending motion of a typical IPMC actuator. (**a**) Before applying voltage. (**b**) After applying voltage

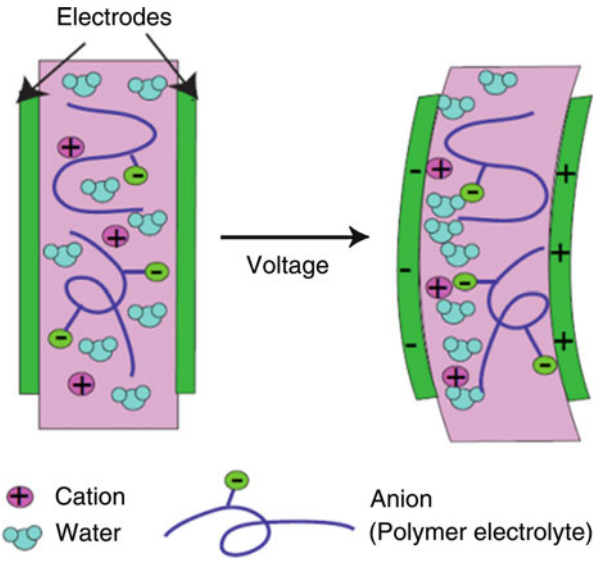

Fig. 2 Schematic view of the bending response mechanism of an IPMC actuator

et al. 1991). Oguro et al. were the first to report the bending response of a perfluorosulfonic acid membrane (Nafion 117) plated with platinum electrodes and activated by low voltages (~1 V) (Oguro et al. 1992). A similar concept was also reported by Shahinpoor (1992). Electromechanical actuators and mechanoelectrical sensors based on IPs were introduced as IPMCs by Shahinpoor et al. (1998). Moreover, in 1999, Fujiwara et al. developed Nafion/gold IPMCs (Fujiwara et al. 1999). The first comprehensive reviews of IPMCs (Shahinpoor and Kim 2001, 2004, 2005; Kim and Shahinpoor 2003) suggested that they are more durable and exhibit higher responses than any other electric response of polymer gels. Hence, many researchers have investigated IPMC actuators and sensors for use in various applications. Recently, several articles on EAPs, including reviews, as well as a review article on IPMCs have been published (Kim and Tadokoro 2007; Shahinpoor et al. 2007; Carpi and Smela 2009; Jo et al. 2013; Asaka and Okuzaki 2014).

In the following sections, configurations of IPMC devices, including the electrode materials and IPs used, the basic techniques employed for characterizing IPMCs, the electromechanical and mechanical modeling of IPMCs, and their electrochemistry, will be described.

2 Device Configuration

The basic configuration of an IPMC device is shown in Fig. 2. The composite is composed of an IP plated between two metal electrodes. Electrodes play a significant role in the electromechanical coupling of IPMCs. The physical properties of the electrodes, such as their electric conductivity, mechanical durability, and surface morphology, have a significant effect on the actuation performance and reliability of IPMCs. The ideal electrodes for IPMCs should be highly electrically conductive, mechanically compliant, and durable against cyclic deformations and must remain electrochemically inert in corrosive environments (e.g., water) in the presence of an electric potential (~4 V). These design requirements limit the choice of available electrode materials considerably. A variety of electrically conductive materials have been investigated for use as IPMC electrodes, including metals (Pt (Kim and Shahinpoor 2003), Au (Fujiwara et al. 1999), Ag (Chung et al. 2006), Cu–Pt (Johanson et al. 2008), Pd–Pt (Kim and Kim 2008), and Pd (Aoyagi and Omiya 2013)), transition metal oxides (Akle et al. 2006; Kim et al. 2009), conducting polymers (Pasquale et al. 2014), and various carbon derivatives such as carbon nanotubes (Levitsky et al. 2004), graphene (Lu et al. 2013), and nanoporous activated and carbide-derived carbons (Palmre et al. 2011; Vunder et al. 2014).

There are two main methods for plating the electrodes for IPMCs. The most widely investigated IPMC electrode materials are Pt (Kim and Shahinpoor 2003) and Au (Fujiwara et al. 1999). The electrodes can be plated by a chemical plating method, which is a chemical process consisting of three steps: (1) roughening of the surface of the IP by sandblasting or other methods, (2) ensuring the adsorption of the metal complex by immersing the IP in an aqueous solution of the metal complex, and (3) fabricating the metal electrodes on the surface of the IP by reducing the adsorbed metal complex. Another method is the so-called "direct assembly" method, which is a physical loading method (Akle et al. 2006). In this method, first, a dispersing solution consisting of the electrode material and the IP in a suitable solvent is prepared. This solution is then directly coated or sprayed on the surface of the IP surface.

IP membranes also play an important role in determining the actuator performance. In particular, the electrochemomechanical properties of IP membranes, such as their ion-transport properties (ion-exchange capacity, liquid electrolyte uptake, and ionic conductivity) and mechanical properties (tensile modulus, strength, and elongation), must be evaluated carefully, if one wishes to enhance actuator performance.

Perfluorinated polymers, such as Nafion and Flemion, which contain ionic sulfonate and carboxylate groups, respectively, are the most widely investigated IP

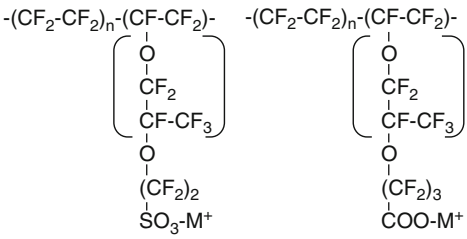

Fig. 3 Chemical structure of fluorinated polymers

materials used in IPMC actuators (Fig. 3) (Asaka and Oguro 2009a). However, these perfluorinated ionomer membranes suffer from a few drawbacks, such as a low actuation bandwidth; low blocking force; low durability; environmental unfriendliness, given that they are fluorinated polymers; and high cost of fabrication, which limit their practical application.

To overcome these problems, a number of synthetic IPs have been proposed. Among these alternative IPs, sulfonated hydrocarbon polymers have received significant attention, owing to their cost effectiveness, ease of fabrication, tunable stiffness, and good ion-transport properties, which result from their controllable monomer composition, especially via the manipulation of the block copolymers. Naturally abundant functional biopolymers such as cellulose derivatives and chitosan have been considered for their high ionic conductivity, environmental friendliness, low cost, and ability to form uniform films. Another solution is to embed functional nanoparticles in a polymer matrix to fabricate a high-performance nanocomposite membrane (Jo et al. 2013).

The counterions and solvents of IPs play an important role in determining the actuator performance. The differences in the properties of the hydrophilic and hydrophobic cations in the perfluorosulfonic acid polymer determine the bending speed and amplitude of the IPMC actuator (Nemat-Nasser and Wu 2003; Asaka and Oguro 2009a). Water is the most widely investigated solvent for IPMC actuators, since the ionic conductivity of IPs in an aqueous environment is usually higher than that in other solvents. In order to develop an IPMC actuator operable in air, an organic solvent and an ionic liquid to be used as a solvent and electrolyte have been developed (Bennett and Leo 2004; Akle et al. 2006; Nemat-Nasser and Zamani 2006; Lee and Yoo 2009; Kikuchi and Tsuchitani 2009; Kikuchi et al. 2011; Lin et al. 2011).

One of the advantages of IPMCs as actuator materials is that they can be readily formed into various shapes, their properties can be engineered, and they can potentially be integrated with microelectromechanical systems-based sensors as control devices to produce smart systems. An IP such as Nafion can be synthesized readily by casting the dispersing solution and evaporating the solvent or by hot molding the thermoplastic resin. The electrodes can also be patterned readily using a PC-controlled mechanical or optical (laser) cutting machine. Therefore, there have many reports on IPMC devices of different shapes and various electrode configurations (Asaka and Oguro 2009b).

3 Characterization of IPMC Actuators

In order to characterize an IPMC actuator, it is necessary to electromechanically characterize it on the basis of actuation and force measurements. These methods are described in ▶ Chap. 10, "IPMCs as EAPs: How to Start Experimenting with Them" of this book. Here, the techniques used to characterize an IP and its plated electrodes are described (Rajagopalan et al. 2010; Wang et al. 2010; Panwar et al. 2012; Wang et al. 2014). These are also important for developing new actuator materials.

Characterizing an IP for an IPMC actuator involves determining its water content, ion-exchange capacity, ionic conductivity, and mechanical properties, as described below.

The water content of an IP is determined by determining the difference in the weights of fully water-equilibrated and vacuum-dried IP samples. One example method is described below:

The surface of the water-equilibrated IP is wiped quickly with absorbent paper, in order to remove any excess water, and the fully hydrated IP is weighed immediately (W_h). The IP is then dried overnight in a vacuum at 80 °C, and the weight of the dried IP (W_d) is then measured. The water content (W_C) of the IP is given by Eq. 1:

$$w_c = \frac{(w_h - w_d)}{w_d}. \tag{1}$$

The ion-exchange capacity of the IP is evaluated using a chemical titration method. One example method is as follows:

First, the IP is immersed in a saturated solution of an electrolyte containing the appropriate counterions overnight, in order to exchange the protons with the counterions. Then, the protons in the solution are titrated against a 0.1 N NaOH solution using phenolphthalein as the indicator.

The ionic conductivity is evaluated through AC impedance measurements. The IP film is sandwiched between two stainless steel electrodes, to which an AC perturbation of low magnitude (e.g., 10 mV_{rms}) with frequencies of 1 Hz to 100 kHz is applied using a complex impedance analyzer. The IP is immersed in deionized water for 24 h before its ionic conductivity is measured. The ionic conductivity, κ, is evaluated using Eq. 2:

$$\kappa = \frac{h}{RS}, \tag{2}$$

where R is the resistance at a limiting high frequency, h is the thickness of the IP film, and the S is the area of the IP film.

The mechanical properties of an IP are determined by evaluating its tensile strength and modulus. Stress/strain measurements are performed on a film of the IP with a cross-sectional area S and length L, and the tensile modulus of the IP is calculated from its initial slope; the tensile strength of the IP is obtained from the strain value at which the IP film breaks.

Dynamical mechanical analysis is also employed to determine the mechanical properties of IPs. The dynamic mechanical properties (storage modulus and loss factor) of an IP are measured using a dynamic mechanical analyzer in the tensile mode. An IP film (rectangular) is used for measuring the dynamic mechanical properties. Frequency sweeps are performed at a small strain or stress at different temperatures. The IPMC sample can also be used to measure the dynamic mechanical properties.

In the case of new IP materials, standard chemical analysis techniques, such as infrared spectroscopy, nuclear magnetic resonance, X-ray photoelectron spectroscopy, and X-ray diffraction analysis, and thermogravimetric analysis and/or standard structural analysis methods, such as scanning electron microscopy (SEM), transmission electron microscopy (TEM), and atomic force microscopy (AFM), are used.

In order to characterize the plated electrodes, their electrical capacitance, conductivity, and mechanical properties must be determined. The electrical capacitance, C_E, of the plated electrodes of an IPMC is estimated using Eq. 3 on the basis of the peak-to-peak charging current, i_d, which is determined from the cyclic voltammogram:

$$C_E = \frac{i_d}{V_o}, \tag{3}$$

where *Vo* is the sweep rate of the applied triangular voltage. Here, it is assumed that the electrical capacitances of the two electrodes are the same.

Cyclic voltammetry (CV) is performed on the IPMC, which is sandwiched by the two electrodes, by applying a triangular voltage.

The electrical conductivity of the plated electrodes is estimated from their sheet resistances, which are measured using a low-resistivity meter with a four-pin probe (measurement range of 10^{-2} to 10^{6} Ω).

The tensile strength and stress of the IPMC are measured in the same manner as those of the IP. The bending stiffness of a fully hydrated IPMC sample is estimated using the free oscillation attenuation method. By bending the sample to the appropriate initial displacement, the free vibration response can be recorded. The natural frequency of the cantilever, f_n, is obtained from the fast Fourier transform of the free vibration response curve. The stiffness of the IPMC, E_{eq}, is determined using Eq. 4, which is based on the thin cantilever beam theory of material mechanics:

$$E_{eq} = \left(\frac{2\pi}{3.515}\right)^2 f_n^2 \frac{l}{L} m l^3 \frac{12}{h^3 t}, \tag{4}$$

where the parameters h, t, m, l, and L represent the thickness, width, weight, and the free and total lengths of the IPMC strip, respectively.

It is also essential to observe the morphologies of the plated electrodes using SEM, TEM, or AFM. Figure 4 shows a SEM image of a cross section of a Pt-plated Nafion 117 membrane. As can be seen from the figure, the morphology of the plated electrodes determines the electrochemical and mechanical properties of the IPMC and thus its electromechanical actuation performance.

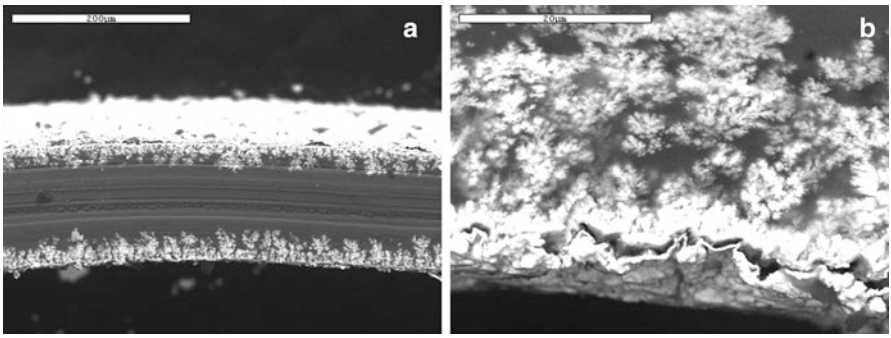

Fig. 4 (**a**) SEM image of a cross section of a typical IPMC thin strip and (**b**) SEM image showing the penetration of the plated metal electrodes in a fractal-like manner around nanoclusters within the material

4 Electromechanical Modeling of IPMCs

The primary objective of modeling IPMCs is to facilitate IPMC fabrication and performance prediction, to understand the underlying principles of IPMC actuation and sensing, and to develop functional real-time control systems for IPMC devices. Subsequent chapters of this book will provide detailed overviews of IPMC modeling with a specific emphasis on physics-based models and control models. The underlying governing equations as well as the methods employed for solving these equations will be discussed. Basically, two types of IPMC actuators models are used: physics-based models and control models. Physics-based models, or white-box models, provide a thorough understanding of the IPMC electromechanical phenomena; however, these models are more complex and often numerical in nature.

This section focuses on physics-based models of IPMCs and compares the contributions made by various research groups. In IPMCs, the underlying causes of electromechanical (actuator) transduction need the study on the transport of ion and water molecule in IPMCs. The electromechanical coupling effect of IPMCs is dependent on the transport of the inner ions and water molecules. First, while focusing on the process of the transport of ions and water in IPMCs, the main aspects of physics-based model are reviewed. Then, the recent developments in static models based on the ion clusters in perfluorinated acid membranes are introduced.

A fundamental physics-based model of IPMCs is shown below; in this model, the phenomena of electromechanical and mechanoelectrical transduction are induced in the IPMC by an ionic current. This results in a nonzero spatial charge in the vicinity of the electrodes. For both cases, the ionic current in the polymer can be described using the Nernst–Planck equation (Pugal et al. 2011, 2013):

$$\frac{\partial C}{\partial t} + \nabla \cdot (-D\nabla C - z\mu FC\nabla\phi - \mu C\Delta V\nabla P) = 0, \tag{5}$$

where C is the cation concentration; μ is the mobility of the cations; D is the diffusion coefficient; F is the Faraday constant; z is the charge number; ΔV is the molar volume, which determines the cation hydrophilicity; P is the solvent pressure; and ϕ is the electric potential in the polymer.

The gradient of the electric potential can be described using Poisson's equation (Pugal et al. 2011, 2013):

$$-\nabla^2\phi = \frac{F\rho}{\varepsilon}, \tag{6}$$

where ε is the absolute dielectric permittivity and ρ is the charge density and is defined as follows:

$$\rho = C - C_a, \tag{7}$$

where C_a is the local anion concentration.

These basic equations form the so-called Poisson–Nernst–Planck (PNP) model for IPMCs and describe the fundamental physics within the polymer membrane. A number of authors have developed electromechanical (actuator) and mechanoelectrical (sensor) models based on the PNP model as well as modified PNP models (Nemat-Nasser 2002; Nemat-Nasser and Zamani 2006; Wallmersperger et al. 2007; Zhang and Yang 2007; Porfiri 2008; Chen and Tan 2008; Aureli et al. 2009). This model will be described further in subsequent chapters of this book.

The underlying causes of transduction in solvent fluxes and ion currents have been discussed previously by several authors. Asaka and Oguro (2000) proposed an IPMC model in which the bending response is attributed to the electroosmosis flow in the ionic gel film by taking into account only the water flow in the membrane. Tadokoro et al. (2000) developed a frictional model, in which the cations together with the hydrated water migrate from the anode to the cathode, owing to the electrostatic force. The electrostatic force is balanced by the frictional force and the diffusion force induced by the concentration gradients. On the other hand, for the free water molecules, the frictional force is solely balanced by the diffusion force. The water flow causes the cathode side to swell, which results in the bending motion of the IPMC. The governing equation is as follows:

$$eE = \eta_I v_I + kT\nabla \ln C_I + n_{dW} kT\nabla \ln C_W, \tag{8}$$

$$kT\nabla \ln C_W = \eta_W v_W, \tag{9}$$

where e is the element charge, k is the Boltzmann constant, v_i is the velocity, and η_i is the viscous resistance coefficient of the ith component.

In the same year, de Gennes et al. (2000) proposed a more comprehensive theory using the standard Onsager relations for the electric current, j_e, and water flux, j_s, based on irreversible thermodynamics:

$$j_e = -\sigma_e \nabla\psi - \lambda\nabla p, \tag{10}$$

$$j_s = -\kappa \nabla p - \gamma \nabla \psi, \tag{11}$$

where σ_e is the conductance, κ is Darcy's permeability, and λ is Onsager's coupling constant. They qualitatively discussed the actuation and sensor properties; however, a quantitative analysis was not performed using these equations.

Yamaue et al. (2005) developed the electrostress diffusion coupling model for describing the deformation dynamics of ion gels under an electric field. This model is a straightforward extension of the stress diffusion coupling model, which was proposed by Doi (2009). By taking into account the coupling of the network stress with the solvent permeation of the gel network and by adding a kinetics equation for the ion flux and electric potential, Yamaue and coworkers could derive a complete set of equations for gel deformation. In this model, the Onsager coefficients, given by Eqs. 10 and 11, are represented by the following microscopic material parameters:

$$\sigma_e = \frac{C_p q_p^2}{\zeta_p} + \sum\nolimits_i \frac{C_i q_i^2}{\zeta_i}, \tag{12}$$

$$\lambda = -\frac{q_p}{\zeta_p}\left(1 - \varnothing_p\right) + \sum\nolimits_i \frac{c_i q_i w_i}{\zeta_i}, \tag{13}$$

$$\kappa = \frac{\left(1 - \varnothing_p\right)^2}{c_p \zeta_p} + \sum\nolimits_i \frac{c_i w_i^2}{\zeta_i}, \tag{14}$$

where the suffixes p, s, and i denote the polymer, solvent, and ions, respectively, and c, q, ζ, and w represent the concentration (number of molecules per unit volume), charge, friction constant related to the solvent, and specific volume, respectively.

Then, the friction constant for the free ions is given by the Stokes–Einstein law:

$$\zeta_i = 6\pi\eta a_i, \tag{15}$$

where η is the viscosity of the solvent and a_i is the ionic radius. Then, the friction constant of the polymer gel, ζ_p, is given by

$$\zeta_p = \frac{6\pi\eta}{\xi_p^2 c_p}, \tag{16}$$

where ξ_b is the diameter of the microhydrophilic channel.

Using Eqs. 15 and 16, the Onsager coefficients can be written as

$$\sigma_e = \frac{c_p q_p^2}{6\pi\eta\xi_b}\left\{c_p \xi_b^3 + \frac{\xi_b}{a_i}\right\}, \tag{17}$$

$$\lambda = \frac{c_p q_p \xi_b^2}{6\pi\eta}\left\{-\left(1 - \varnothing_p\right) - \frac{4\pi}{3}\left(\frac{a_i}{\xi_b}\right)^2\right\}, \tag{18}$$

$$\kappa = \frac{\left(1-\varnothing_p\right)^2 \xi_b^2}{6\pi\eta}\left\{1+\left(\frac{4\pi}{3\left(1-\varnothing_p\right)}\right)^2 c_p \xi_b^3 \left(\frac{a_i}{\xi_b}\right)^3\right\}. \tag{19}$$

Equations 17 and 18 show that the conductivity decreases and the rate of electroosmosis increases as the ion size increases with respect to the channel size. These results have been shown to qualitatively agree with those of displacement experiments (Yamaue et al. 2005). The initial peak curvature, *CUR*, is given by the following equation:

$$CUR = \frac{4}{h^2}\frac{\lambda}{\sigma_e} Q. \tag{20}$$

This suggests that the initial curvature is driven by the pressure gradient caused in the ion gel by the electroosmosis flow. Hence, the initial curvature is a function of the ionic charge, Q, and the water transference coefficient, λ/σ_e, which describes the number of water molecules transferred per counter cation transferred. The experimentally determined initial curvature of an IPMC actuator (Nafion 117/Au) having various ionic forms could be reproduced with fidelity using the theoretical curves described by Eqs. 17, 18, and 20 (Yamaue et al. 2005).

Recently, Zhu et al. (2013a, b) developed a physics-based IPMC model using the extended Nernst–Planck equation, which takes into the coupling effects, as follows:

$$J_i = -d_{II}\left(\nabla c_I + \frac{z_I F c_I}{RT}\nabla\varnothing + \frac{\overline{V}_I c_I}{RT}\nabla p\right) - n_{dI} d_{WW}\left(\nabla c_W + \frac{\overline{V}_W c_W}{RT}\nabla p\right) - c_I K \nabla p, \tag{21}$$

$$J_w = -d_{WW}\left(\nabla c_W + \frac{\overline{V}_W c_W}{RT}\nabla \mathrm{p}\right) - n_{dW} d_{II}\left(\nabla c_I + \frac{z_I F c_I}{RT}\nabla\varnothing + \frac{\overline{V}_I c_I}{RT}\nabla p\right) - c_W K \nabla p. \tag{22}$$

By solving Eqs. 21 and 22 and by coupling them with the Poisson equation (Eq. 6) and the continuity equation (Eq. 23) using a computational method, the redistribution of the cations and water in response to the applied voltage could be calculated:

$$\frac{\partial c_i}{\partial t} + \nabla J_i = 0 \quad (i = \mathrm{I},\ \mathrm{W}). \tag{23}$$

Based on the ion-cluster model of the perfluorosulfonic acid polymer, shown in Fig. 5, the change in the concentration of the cations and water transfer into those which are calculated by Eqs. 21, 22, and 23 results in the pressure state in the cluster by using the following relations:

$$\sigma_{eB} - \sigma_{eA} = \frac{E_{\mathrm{dry}}}{3}\left(\left(\frac{1+w_v}{1+w_{vo}}\right)^{-4/3} - \left(\frac{w_v}{w_{vo}}\right)^{-4/3}\right), \tag{24}$$

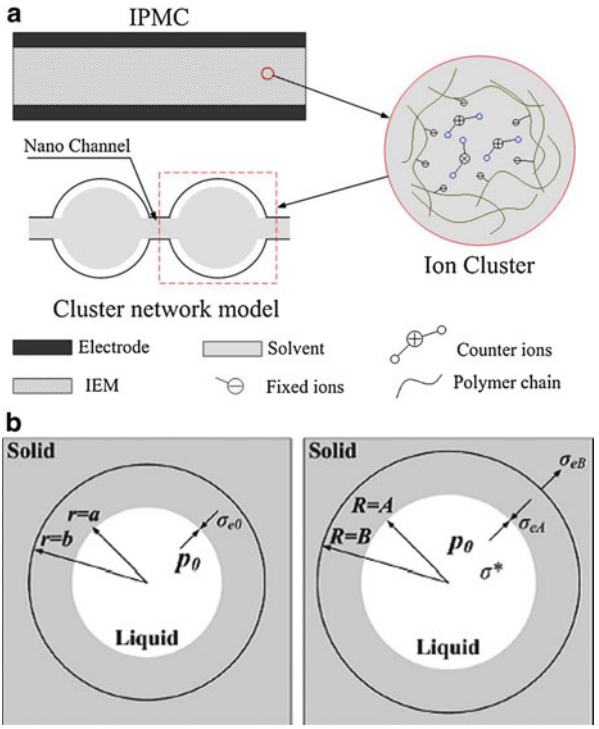

Fig. 5 Ion-cluster model of a perfluorosulfonic acid-based IPMC. (**a**) Ion-cluster network mode and (**b**) schematic view of the stress valance in the ion cluster (Reproduced from Zhu et al. 2013a)

where σ_{eB} and σ_{eA} are the external and internal stresses of the ion cluster, respectively (Fig. 5b); E_{dry} is the elastic modulus of the dry polymer; and w_v and w_{vo} are the volume fraction and initial volume fraction of the water in the ionic polymer, respectively (Zhu et al. 2013a, b).

The hydrostatic pressure of the ion cluster is given by

$$p_h = -\sigma_{eA}. \tag{25}$$

By adding the osmotic pressure, Π, the electrostatic stress, p_e, and the capillary pressure, Π_σ (eigenstresses), in the ion cluster, which are induced by the redistribution of the ions and water, the total internal pressure, p, of the ion cluster can be calculated (Zhu et al. 2013a, b):

$$p = p_h + \Pi_\sigma - \Pi - p_e. \tag{26}$$

By establishing the above model, Zhu et al. could successfully describe the complicated deformation behaviors of the IPMC under various conditions (Zhu et al. 2013a, b).

5 Electrochemistry of IPMCs

The standard AC impedance technique is a powerful tool for exploring the electrochemical properties of IPMCs, as it can be used to determine their equivalent electric circuits.

It is assumed that the IPMC is composed of an IP film sandwiched between two perfectly conductive metal electrodes. The linearized PNP model is used to describe the dynamics of the electric potential and the concentration of the mobile counterions within the polymer. In the case of the flat electrodes, by solving the partial differential equation based on the PNP model, the equivalent circuit, which is composed of the following lumped capacitances – the double-layer capacitance, C_d, the bulk capacitance C_b, and the bulk conductance, S_b (see Fig. 6a) – can be obtained (Aureli and Porfiri 2012).

The chemical (electroless) plating process for plating the metal electrodes, which has been described previously, is typically repeated several times, in order to increase the thickness and hence the electric conductivity of the electrode layers. The sequential plating steps result in a dendrite-like structure in the electrode layer; this structure penetrates into the ionic polymer, as shown in Fig. 4. In such a case, the interface between the IP and the electrode is rough. Further, the equivalent circuit of the IPMC is a distributed circuit composed of a capacitance, *C(r)*, and a conductance, *S(r)*, as shown in Fig. 6b (Aureli and Porfiri 2012).

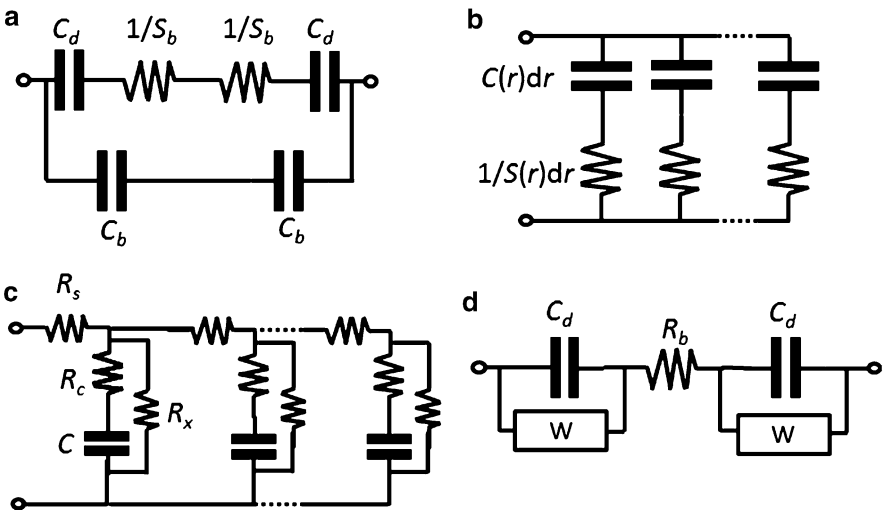

Fig. 6 Equivalent circuits of the IPMC. (**a**) Lumped capacitance and resistance model. (**b**) Distributed circuit model that takes into account the roughness of the plated electrodes. (**c**) A possible distributed circuit model that takes into account the surface resistance of the plated electrodes. (**d**) A possible circuit model that takes into account the ion transport in the porous electrodes

The above discussion assumes that the plated electrodes are perfectly conductive. However, the actual resistance of the plated electrodes is not negligible. When considering the surface resistance of the plated electrodes, several authors have proposed the distributed equivalent circuit shown in Fig. 6c (Shahinpoor and Kim 2000; Paquette et al. 2003; Punning et al. 2007; Chen and Tan 2008). In this figure, C is the distributed element of the double-layer capacitance, R_c is that of the electrolyte resistance, R_s is that of the surface resistance of the electrode, and R_x is the shunt resistance.

The electrode layers formed using the physical loading method are usually relatively thicker (more than 10 μm in thickness), and the composite layers are composed of nanoparticles of the electrode material and the ionic polymer. These layers are both electronically and ionically conductive. The impedance for such electrodes is assumed to be similar to that of porous electrodes. Levie (1963, 1964) was the first to develop a transmission line circuit (TLC) model of the porous electrode consisting of the electrolyte resistance and the double-layer capacitance. Subsequently, a number of authors proposed modified TLC models for the impedance of porous electrodes on the basis of Levie's model. Bisquert (2000) reviewed the various impedance models for porous electrodes. The composite electrode layers prepared by the physical loading method could be successfully represented by the impedance model for porous electrodes, as shown in Fig. 6d; this model is composed of the double-layer capacitance, C_d; the Warburg diffusion capacitance, W; and the electrolyte resistance, R_b (Liu et al. 2012; Cha and Porfiri 2013).

Another important tool for electrochemical analysis is CV, which is used for estimating the double-layer capacitance of the electrode layer, as described in Sect. 3. CV is the standard electrochemical technique for studying the electrode reactions (Bard and Falkner 2001). The redox reactions involving the Pt, Au, and Pd electrodes used in IPMCs have been studied using CV, and the obtained results have been discussed with respect to the displacement behavior (Asaka and Oguro 2000; Kim et al. 2011; Aoyagi and Omiya 2013). Figure 7 shows the results of CV and displacement measurements for a Pt-IPMC in an H_2SO_4 solution. It can be seen clearly that the displacement direction is regulated by the redox reaction of the Pt electrodes. When coupled with the phenomena occurring in IPs (see Sect. 5), the dependence of the displacement behavior of the IPMC on the various parameters, such as the amplitude of the applied voltage, the IP species, the electrode materials, the counterion species, the pH level, and the water content, becomes complex.

6 Mechanical Properties of IPMCs

As has been described previously, IPMCs bend toward the cathode or anode (depending on whether a cation- or anion-exchange polymer is used) under the influence of an applied voltage, owing to the migration of the counterions with solvent molecules. This results in a pressure gradient and difference in the bending

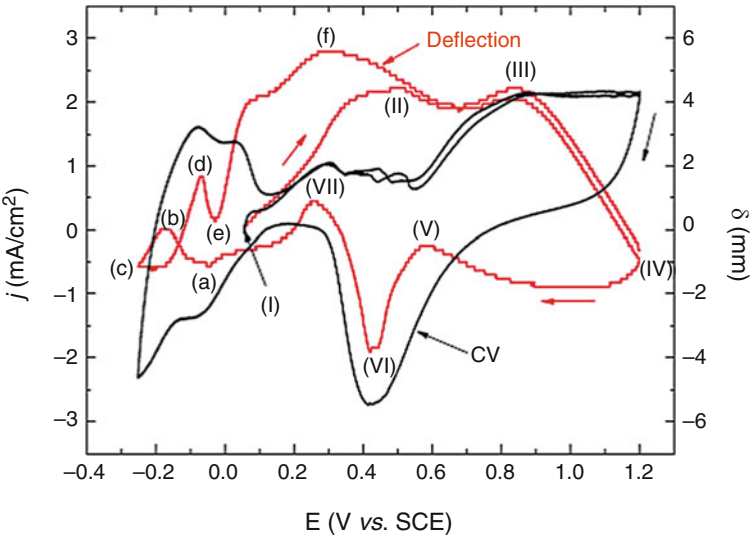

Fig. 7 Results of cyclic voltammetry (CV) and displacement measurements (deflection) performed on the Pt electrode of an IPMC actuator in an H_2SO_4 solution (Reproduced from Kim et al. 2011)

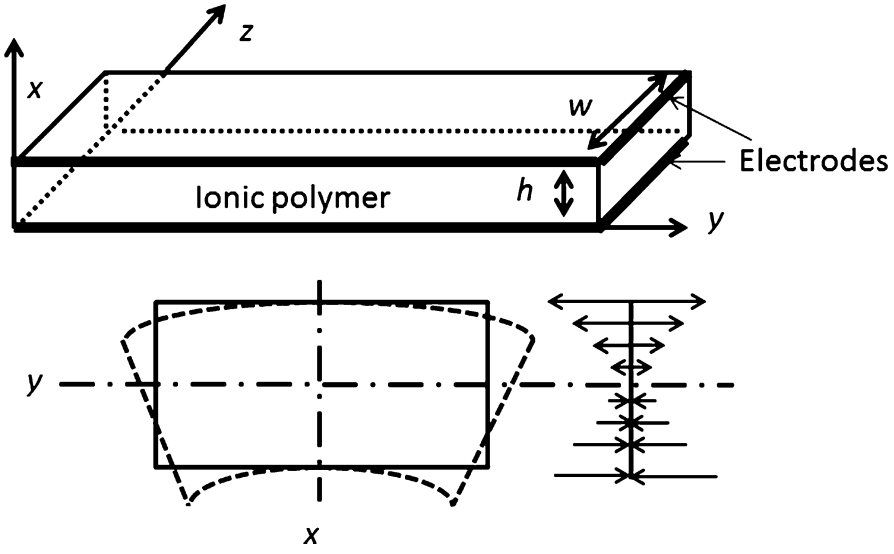

Fig. 8 Stress distribution in an IPMC along the thickness direction

stress between the two sides of the membrane. The situation is similar to that related to the stress distribution caused by the moment, as shown in Fig. 8 (He et al. 2011).

In this case, the bending moment, M, along the z-axis is given by the following equation:

$$M = \int_{o}^{h} \sigma(x,t) w x dx, \tag{27}$$

where w is the width of the IPMC and σ (x, t) is the stress distribution along the thickness direction.

According to the Euler–Bernoulli law, the curvature of the IPMC actuator, CUR, at zero load while assuming that the actuator is perfectly homogeneous along the z-axis is given by

$$CUR = \frac{M}{EI}, \tag{28}$$

where E is the Young modulus of the IPMC actuator and I (=2/3 Wh^3) is the second moment of inertia of the IPMC.

Further, the blocking force of the IPMC, F, is given by

$$F = \frac{M}{L}, \tag{29}$$

where L is the distance of the IPMC actuator.

Therefore, the curvature of the IPMC at load F is given by the following equation:

$$CUR = \frac{M - FL}{EI}, \tag{30}$$

The displacement, δ, can be related to the curvature by the following equation:

$$CUR = \frac{2\delta}{L^2 + \delta^2} \cong \frac{2\delta}{L^2}, \tag{31}$$

The bending moment, M, is a function of the time, t, and the applied voltage, V, and can be derived from electromechanical and electrochemical models described in Sects. 6 and 7. The mechanical model described here is most basic one and assumes that the IPMC is homogeneous. More rigorous models are described in subsequent chapters of this book.

7 Conclusions

Since the initial reports on IPMCs, significant advances have been made in the development of IPMC actuators and sensors. Electrodes play a significant role in determining the degree of electromechanical coupling in IPMCs. A variety of electrically conductive materials have been investigated for use for IPMC electrodes, including metals, transition metal oxides, conducting polymers, and various carbon derivatives. IP membranes also play an important role in determining the actuator

performance. Perfluorinated polymers, such as Nafion and Flemion, which contain ionic sulfonate and carboxylate groups, respectively, are the most widely investigated IP materials used in IPMC actuators. However, these perfluorinated ionomer membranes suffer from a few drawbacks, such as a low actuation bandwidth; low blocking force; low durability; environmental unfriendliness, given that they are fluorinated polymers; and high cost of fabrication, which limit their use in practical applications. To overcome these problems, a number of synthetic IPs have been proposed.

The various techniques used to characterize IPs and plated electrodes were described, as these are also important for developing new actuator materials.

This chapter focused on physics-based models of IPMCs and compared the contributions made by various research groups. In IPMCs, the underlying causes of electromechanical (actuator) transduction need the study on the transport of ion and water molecule in IPMCs. The electromechanical coupling effect of IPMCs is dependent on the transport of the inner ions and water molecules. In this chapter, while focusing on the transport process of ions and water in IPMCs, physics-based models of IPMCs were reviewed. Further, the recent developments in static models based on the ion-cluster structure of perfluorinated acid membranes were introduced.

In the last two sections of this chapter, the basics of the electrochemistry of IPMCs and their mechanical modeling were discussed.

Given the recent developments in the materials used for IPMCs and owing to the elucidation of the working principles of IPMC actuators and sensor, IPMCs are increasingly being used in various biomedical applications, including in biomimetic robotics and sensor/actuator integration, and for energy harvesting.

References

Akle BJ, Bennett MD, Leo DJ (2006) High-strain ionomeric-ionic liquid electroactive actuators. Sens Actuators A 126:173–181

Aoyagi W, Omiya M (2013) Mechanical and electrochemical properties of an IPMC actuator with palladium electrodes in acid and alkaline solutions. Smart Mater Struct 22:055028 (10 pp)

Asaka K, Oguro K (2000) Bending of Polyelectrolyte Membrane-platinum composites by electric stimuli. Part II. Response kinetics. J Electroanal Chem 480:186–198

Asaka K, Oguro K (2009a) IPMC actuators: fundamentals. In: Carpi F, Smela E (eds) Biomedical applications of electroactive polymer actuators. Wiley, Chichester, pp 103–119

Asaka K, Oguro K (2009b) Active microcatheter and biomedical soft devices based on IPMC actuators. In: Carpi F, Smela E (eds) Biomedical applications of electroactive polymer actuators. Wiley, Chichester, pp 103–119

Asaka K, Okuzaki H (eds) (2014) Soft actuators – material, modeling, applications and future perspectives. Springer, Tokyo

Aureli M, Porfiri M (2012) Effect of electrode surface roughness on the electrical impedance of ionic polymer–metal composites. Smart Mater Struct 21:105030

Aureli M, Lin W, Porfiri M (2009) On the capacitance-boost of ionic polymer metal composites due to electroless plating: theory and experiments. J Appl Phys 105:104911

Bard AJ, Falkner LF (2001) Electrochemical methods: fundamentals and applications, 2nd edn. Wiley, New York

Bennett MD, Leo DJ (2004) Ionic liquids as stable solvents for ionic polymer transducers. Sens Actuators A-Phys 115:79–90
Bisquert J (2000) Influence of the boundaries in the impedance of porous film electrodes. Phys Chem Chem Phys 2:4185–4192
Carpi F, Smela E (eds) (2009) Biomedical applications of electroactive polymer actuators. Wiley, Chichester
Cha Y, Porfiri M (2013) Bias-dependent model of the electrical impedance of ionic polymer-metal composites. Phys Rev E 87:022403
Chen Z, Tan X (2008) A control-oriented and physics-based model for ionic polymer-metal composite actuators. IEEE/ASME Trans Mechatron 13(5):519–529
Chung CK, Fung PK, Hong YZ et al (2006) A novel fabrication of ionic polymer-metal composites (IPMC) actuator with silver nano-powders. Sens Actuators B 117:367–375
de Gennes PG, Okumura K, Shahinpoor M, Kim KJ (2000) Mechanoelectric effects in ionic gels. Europhys Lett 50:513–518
de Levie R (1963) On porous electrodes in electrolyte solutions: I. Capacitance effects. Electrochim Acta 8:751–780
de Levie R (1964) On porous electrodes in electrolyte solutions—IV. Electrochim Acta 9:1231–1245
DeRossi D, Kajiwara K, Osada Y, Yamauchi A (eds) (1991) Polymer gels – fundamentals and biomedical applications. Plenum Press, New York
Doi M (2009) Gel dynamics. J Phys Soc Jpn 78(5): 052001
Fujiwara N, Asaka K, Nishimura Y et al (1999) Preparation of gold-solid electrolyte composites as electric stimuli responsive materials. Chem Mater 12:1750–1754
Hamlen RP, Kent CE, Shafer SN (1965) Electrolytically activated contractile polymer. Nature 206:1149–1150
He Q, Yu M, Song L et al (2011) Experimental study and model analysis of the performance of IPMC membranes with various thickness. J Bionic Eng 8:77–85
Jo CH, Pugal D, Oh IK et al (2013) Recent advances in ionic polymer-metal composite actuators and their modeling and applications. Prog Polym Sci 38(7):1037–1066
Johanson U, Maeorg U, Sammelselg V et al (2008) Electrode reactions in Cu-Pt coated ionic polymer actuators. Sens Actuators B 31:340–346
Kikuchi K, Tsuchitani S (2009) Nafion based polymer actuators with ionic liquids as solvent incorporated at room temperature. J Appl Phys 106:053519
Kikuchi K, Sakamoto T, Tsuchitani S et al (2011) Comparative study of bending characteristics of ionic polymer actuators containing ionic liquids for modeling actuation. J Appl Phys 109:073505
Kim SM, Kim KJ (2008) Palladium buffer-layered high performance ionic polymer-metal composites. Smart Mater Struct 17:035011
Kim KJ, Shahinpoor M (2003) Ionic polymer-metal composites – II. Manufacturing techniques. Smart Mater Struct 12:65–79
Kim KJ, Tadokoro S (eds) (2007) Electroactive polymers for robotics applications. Springer, London
Kim SM, Tiwari R, Kim KJ (2009) A novel ionic polymer-metal composites incorporating ZnO thin film. Smart Mater Struct Electroactive Polym Actuators Devices 7287:72870W-1-7
Kim D, Kim KJ, Nam JD et al (2011) Electro-chemical operation of ionic polymer–metal composites. Sens Actuators B 155(2011):106–113
Lee JW, Yoo YT (2009) Anion effects in imidazolium ionic liquids on the performance of IPMCs. Sens Actuators B 137:539–546
Levitsky IA, Kanelos P, Euler WB (2004) Electromechanical actuation of composite material from carbon nanotubes and ionomeric polymer. J Chem Phys 121:1058–1165
Lin J, Liu Y, Zhang QM (2011) Charge dynamics and bending actuation in Aquivion membrane swelled with ionic liquids. Polymer 52:540–546
Liu Y, Zhao R, Ghaffari M et al (2012) Equivalent circuit modeling of ionomer and ionic polymer conductive network composite actuators containing ionic liquids. Sens Actuators A 181:70–76

Lu L, Liu J, Zhang Y et al (2013) Graphene-stabilized silver nanoparticle electrochemical electrode for actuator design. Adv Mater 25:1270–1274
Nemat-Nasser S (2002) Micromechanics of actuation of ionic polymer-metal composites. J Appl Phys 92:2899–2915
Nemat-Nasser S, Wu Y (2003) Comparative experimental study of ionic polymer-metal composites with different backbone ionomers and in various cation forms. J Appl Phys 93:5255–5267
Nemat-Nasser S, Zamani S (2006) Modeling of electrochemomechanical response of ionic polymer-metal composites with various solvents. J Appl Phys 100:064310
Oguro K, Kawami Y, Takenaka H (1992) Bending of an ion-conducting polymer film-electrode composite by an electric stimulus at low voltage. J Micromach Soc 5:27–30
Palmre V, Lust E, Janes A et al (2011) Electroactive polymer actuators with carbon aerogel electrodes. J Mater Chem 21:2577–2583
Panwar V, Lee C, Ko SY et al (2012) Dynamic mechanical, electrical, and actuation properties of ionic polymer metal composites using PVDF/PVP/PSSA blend membranes. Mater Chem Phys 135:928–937
Paquette JW, Kim KJ, Nam JD et al (2003) An equivalent circuit model for ionic polymer-metal composites and their performance improvement by a clay-based polymer nano-composite technique. J Intell Mater Syst Struct 14:633–642
Pasquale GD, Graziani S, Messina FG et al (2014) An investigation of the structure–property relationships in ionic polymer polymer composites (IP2Cs) manufactured by polymerization in situ of PEDOT/PSS on Nafion R 117. Smart Mater Struct 23:035018 (12pp)
Porfiri M (2008) Charge dynamics in ionic polymer metal composites. J Appl Phys 104:104915
Pugal D, Kim KJ, Aabloo A (2011) An explicit physics-based model of ionic polymer-metal composite actuators. J Appl Phys 110(8):084904
Pugal D, Solin P, Aabloo A, Kim KJ (2013) IPMC mechanoelectric transduction: its scalability and optimization. Smart Mater Struct 22(12):125029
Punning A, Kruusmaa M, Aabloo A (2007) Surface resistance experiments with IPMC sensors and actuators. Sens Actuators A 133:200–209
Rajagopalan M, Jeon JH, Oh IK (2010) Electric-stimuli-responsive bending actuator based on sulfonated polyetherimide. Sens Actuators B 151:198–204
Shahinpoor M (1992) Conceptual design, kinematics and dynamics of swimming robotic structures using ionic polymeric gel muscles. Smart Mater Struct 1:91–94
Shahinpoor M, Kim KJ (2000) The effect of surface-electrode resistance on the performance of ionic polymer-metal composite (IPMC) artificial muscles. Smart Mater Struct 9:543–551
Shahinpoor M, Kim KJ (2001) Ionic polymer-metal composites – I. Fundamentals. Smart Mater Struct 10:819–833
Shahinpoor M, Kim KJ (2004) Ionic polymer-metal composites – III. Modeling and simulation as biomimetic sensors, actuators, transducers and artificial muscles. Smart Mater Struct 13:1362–1388
Shahinpoor M, Kim KJ (2005) Ionic polymer-metal composites – IV. Industrial and mechanical applications. Smart Mater Struct 14:197–214
Shahinpoor M, Bar-Cohen Y, Simpson JO, Smith J (1998) Ionic polymer-metal composites (IPMCs) as biomimetic sensors, actuators and artificial muscles-a review. Smart Mater Struct 7:R15–R30
Shahinpoor M, Kim KJ, Mojarrad M (2007) Artificial muscles – applications of advanced polymeric nanocomposites. CRC Press, New York/London
Tadokoro S, Yamagami S, Takamori T et al (2000) Modeling of nafion-Pt composite actuators (ICPF) by ionic motion. Smart Mater Struct Electroactive Polym Actuators Devices 3987:92–102
Vunder V, Itik M, Poldsalu I et al (2014) Inversion based control of ionic polymer–metal composite actuators with nanoporous carbon based electrodes. Smart Mater Struct 23:025010
Wallmersperger T, Leo DJ, Kothera CS (2007) Transport modeling in ionomeric polymer transducers and its relationship to electromechanical coupling. J Appl Phys 101:024912

Wang XL, Oh IK, Lee S (2010) Electroactive artificial muscle based on crosslinked PVA/SPTES. Sens Actuators B 150:57–64

Wang Y, Zhu Z, Chen H et al (2014) Effects of preparation steps on the physical parameters and electromechanical properties of IPMC actuators. Smart Mater Struct 23:125015

Yamaue T, Mukai H, Asaka K, Doi M (2005) Electrostress diffusion coupling model for polyelectrolyte gels. Macromolecules 38:1349–1356

Zhang L, Yang Y (2007) Modeling of an ionic polymer–metal composite beam on human tissue. Smart Mater Struct 16:S197–S206

Zhu Z, Asaka K, Chang L et al (2013a) Multiphysics of ionic polymer-metal composite actuator. J Appl Phys 114:084902

Zhu Z, Asaka K, Chang L et al (2013b) Physical interpretation of deformation evolvement with water content of ionic polymer-metal composite actuator. J Appl Phys 114:184902